1634–1644 *Nucleic Acids Research, 2008, Vol. 36, No. 5* *Published online 3 February 2008*
doi:10.1093/nar/gkn019

Deadenylation-independent stage-specific mRNA degradation in *Leishmania*

Simon Haile, Aurélien Dupé and Barbara Papadopoulou*

Research Centre in Infectious Diseases, CHUL Research Centre and Department of Medical Biology, Faculty of Medicine, Laval University, Quebec, Canada

Received December 4, 2007; Revised and Accepted January 10, 2008

ABSTRACT

The life cycle of *Leishmania* alternates between developmental forms residing within the insect vector (e.g. promastigotes) and the mammalian host (amastigotes). In *Leishmania* nearly all control of gene expression is post-transcriptional and involves sequences in the 3′-untranslated regions (3′UTRs) of mRNAs. Very little is known as to how these *cis*-elements regulate RNA turnover and translation rates in trypanosomatids and nothing is known about mRNA degradation mechanisms in *Leishmania* in particular. Here, we use the amastin mRNA—an amastigote-specific transcript—as a model and show that a ~100 nt U-rich element (URE) within its 3′UTR significantly accounts for developmental regulation. RNase-H-RNA blot analysis revealed that a major part of the rapid promastigote-specific degradation of the amastin mRNA is not initiated by deadenylation. This is in contrast to the amastin mRNA in amastigotes and to reporter RNAs lacking the URE, which, in common with most eukaryotic mRNAs studied to-date, are deadenylated before being degraded. Moreover, our analysis did not reveal a role for decapping in the stage-specific degradation of the amastin mRNA. Overall, these results suggest that degradation of the amastin mRNA of *Leishmania* is likely to be bi-phasic, the first phase being stage-specific and dependent on an unusual URE-mediated pathway of mRNA degradation.

INTRODUCTION

Parasitic species belonging to the kinetoplastid group of protozoans are of high medical and veterinary importance mainly in tropical and subtropical countries. These include trypansomatids such as *Leishmania* spp. (Leishmaniasis), *Trypanosoma brucei* (Sleeping sickness) and *Trypanosoma cruzi* (Chagas disease). Their life cycle involves a mammalian host and an arthropod vector. The parasites face disparate conditions during their life cycle, a drastic change in temperature between their insect (~20–25°C) and mammalian (37°C) hosts being typically a shared challenge. Other changes can be unique to the life style of a given parasite (e.g. the acidic pH that *Leishmania* spp. face within the phagolysosomes of host macrophages). The parasites employ various adaptive strategies to be able to survive and grow in their distinct niches. These stage- or species-specific structural and metabolic adaptations are associated with significant changes in gene expression as evidenced by recent functional genomic analyses [Rochette *et al*., unpublished data; (1–4)].

Kinetoplastids branched very early from the eukaryotic lineage and perhaps because of these they display several unusual or unique biological features. Tens to hundreds of genes are collinearly transcribed into a polycistronic mRNAs (5–7). Individual mRNAs are resolved from nuclear pre-mRNAs via coupled co-transcriptional processes of *trans*-splicing and 3′-end cleavage/polyadenylation (8). The process of *trans*-splicing involves the addition of ~40-bases long capped mini-exon to the 5′-termini of all mRNAs from a separate RNA substrate (*SL-RNA*) [reviewed in (8)]. Transcription has been postulated to initiate at strand switch regions on each chromosome probably within the intercistronic regions (9,10). There is, however, no indication for specific RNA polymerase II promoters associated with protein-coding genes to-date and the genomes of the parasites are short of genes encoding major transcription factors and co-activators. Consequently, most of gene regulation in these parasites occurs at the post-transcriptional levels, mainly via mRNA stability and translation [reviewed in (11,12)].

Eukaryotic mRNAs are typically capped at their 5′-ends and possess poly(A) tail at their 3′-ends. Such modifications at the mRNA termini, plus the proteins they bind to, confer mRNA stability and translatability. The degradation of eukaryotic mRNA is typically triggered by poly(A) tail shortening [reviewed in (13)]. Deadenylation, in turn, invokes decapping and the cumulative outcome is unprotected ends that are readily attacked by 5′- and

*To whom correspondence should be addressed. Tel: +1 418 654 2705; Fax: +1 418 654 2715; Email: barbara.papadopoulou@crchul.ulaval.ca

3′-exonucleases [reviewed in (13,14)]. Two 5′-exonucleases have been identified in yeast, the nuclear Rat1p/Xrn2p and the cytoplasmic Xrn1p (15,16). More than 10 conserved 3′-exonucleases have been characterized and some, together with other protein factors, are found in a complex called the exosome. Besides their role in determining mRNA half-lives in the cytoplasm, the 3′- and 5′-exonucleases are also involved in pre-mRNA quality control and the maturation of ribosomal, nuclear and small nucleolar RNAs [for examples see (17–19)]. In yeast, degradation from the 5′-end seems to be the major determinant of mRNA degradation and the 3′-pathway is only detectable in mutants of the 5′-pathway [reviewed in (13)]. In mammals, there is a growing consensus that both pathways are probably significant determinants of mRNA degradation (20–22).

The genomes of trypanosomes harbor genes that encode for deadenylases [reviewed in (11)]. A clear orthologue of a decapping enzyme has so far proven to be elusive even though decapping activity has been detected in the related organism *Leptomonas seymouri* (23). Degradation of mRNAs in *T. brucei* involves both 5′- and 3′-pathways (24) and homologues of all major 3′-exonucleases (25–27), and 5′-exonucleases (28) are well-characterized. Trypanosome 3′-exonucleases are also found in a complex and display all major RNA processing and degradation functions associated with their counterparts in other eukaryotes (25,26,29,30). Trypanosomes harbor four homologues of Xrn1p and Xrn2p/Rat1p (28). One of these, termed XRNA, is cytoplasmic and has been shown to be critical in the degradation of both stable and unstable mRNAs in *T. brucei* (28).

mRNA degradation *cis* determinants are predominantly found in the 3′-untranslated regions (UTRs) in all three species of trypanomatids. In *Leishmania*, in contrast to other trypansomatids, several hundred of the 3′UTR *cis*-elements belong to two major classes of short interspersed degenerate retroposons, SIDER1 and SIDER2 (31), and several lines of evidence indicate that these elements modulate post-transcriptional gene expression in this parasite (31–33). These elements are thought to have evolved specifically in the *Leishmania* lineage perhaps under the selective pressure presented by the parasite′s unique niches. Whether or not the mechanisms through which these elements function are also unique remains to be determined. The degradation of several unstable mRNAs in *T. brucei* [reviewed in (11) and *T. cruzi* (34)] is dependent on U-rich elements (UREs). These elements seem to be structurally (35) and functionally (24,29,36–40) similar to the mammalian AU-rich elements (AREs) found in several proto-oncogene and inflammatory cytokine mRNAs (41). These elements confer instability in a number of mRNAs in procyclic trypanosomes, developmental forms of the parasite that reside in the mid-gut of the insect vector. In *T. cruzi*, protein factors (UBPs) that bind these elements with high affinity and avidity have been identified (34,42,43). Homologues of these RNA-binding proteins also exist in *T. brucei* even though these proteins seem to have broad RNA-binding specificity (44). No UREs have been reported in *Leishmania* so far and virtually nothing is known about mechanisms underlying mRNA degradation in these parasites. In this study, we demonstrate URE-mediated degradation of the stage-specific amastin mRNA in *Leishmania*, thereby embark on attempts to gain insight into the mechanistic basis of mRNA degradation in this organism.

MATERIALS AND METHODS

Plasmids

The parental plasmid used in this study, pSPBT1-YNEOαLUC, was previously described (33). This plasmid allows the integration of reporter constructs into the *BT1* genomic locus. Sequence corresponding to the amastin (LinJ34_V3.1030) 3′UTR and downstream intergenic region was amplified by PCR from *L. infantum* LEM 1317 genomic DNA (gDNA) using the forward primer, amastin-3′UTR-F (5′-AAGCTACTTCGGATCCGCGG-3′) and the reverse primer, amastin-IR-R (5′-GGATCCGGCTCGCCAGTGTAGCAGAA-3′). The URE deletion construct was made by fusion PCR as described (45). Primers amastin-3′UTR-F and amastin-Up-URE-R (5′-CGTCCATGCGGCTCTTCTCTGCGCGTGCGTGTGTGTCG-3′) were used to amplify the upstream region from the URE. Primers amastin-Down-URE-F (5′-CGACACACACGCACGCGCAGAGAAGAGCCGCATGGACG-3′) and amastin-IR-R, was used to amplify the downstream region of the URE. Primer amastin-Up-URE-R is the reverse complement of primer amastin-Down-URE-F. One hundred nanograms of the resulting PCR products, together with primers Amastin-3′UTR-F and amastin-IR-R, were used for a fusion PCR to generate amastin 3′UTR△URE. The only difference between full-length 3′UTR and 3′UTR-ΔURE is, therefore, the deletion of the 100-nt long URE. The resulting PCR fragments were digested with *Bam*HI (primers amastin-3′UTR-F and amastin-IR-R contain this site) and cloned into the *Bam*HI site of the pSPBT1-YNEOαLUC plasmid, downstream of the firefly luciferase (*LUC*) open reading frame (Figure 2).

Parasite culture and transfections

Leishmania donovani infantum MHOM/MA/67/ITMAP-263, the parental strain for all the parasite lines employed in this study, was cultured in SDM-79 medium (pH 7), supplemented with 10% heat-inactivated fetal calf serum (Multicell, Wisent Inc.) and 5 mg/ml hemin at 25°C as promastigotes and were switched to MAA/20 medium (pH 5.8) at 37°C with 5% CO_2 and passed ~2–3 times to generate axenic amastigotes (46). For genomic integration into the *BT1* locus, ~2.5 μg of *Hpa*I-*Hin*dIII digests (these enzymes only cut on either side of the *BT1* targeting regions) were transfected into promastigote *L. infantum* by electroporation as described (47). Transfected cells were plated on SDM-79 medium with 1.5% agar and 0.01 mg/ml of G418 (Sigma), and individual clones were obtained after 2–3 weeks.

RNA analysis

Parasites were treated with 0.5 μg/ml Actinomycin-D (Sigma) with/without 2.5 μM Sinefungin (Sigma) for mRNA decay rate determination. All time points include 5 min of centrifugation times. Total RNA was extracted from cultures with OD_{600nm} = 0.3–0.5 after lysis with Trizol (Invitrogen) according to the manufacturer's instructions. Ten to forty micrograms RNA was used for standard RNA blotting. Hybridization was done at 42°C with 50% formamide solution and RNA gels were transfered into Hybond-N membranes (Amersham Biosciences) by upward capillary movement. RNase-H (Invitrogen) digestions were carried out as described with 20–60 μg RNA as a starting material (48) in the presence of a specific oligonucleotide 300R (5′-TTGTCTCCGTT CCTCC GGGATCCCG-3′) with or without oligo dT (Invitrogen) and the reaction contained RNase inhibitor (Invitrogen). RNase H samples were run typically on 25 cm × 20 cm, 2–2.4% agarose gels. Polyacrylamide gels were 5% and transfer was carried out using BioRad's submarine system. Blots were probed with a fragment corresponding the last 300 bases of the amastin mRNA. Ten to twenty micrograms RNA was used as a starting material for the Terminator (Epicentre Biotechnologies) treatments of RNA samples. The reactions were carried out according to manufacturer's instructions at 30°C for 1–1.5 h and an RNase inhibitor (Invitrogen) was included in the reaction. Minus Terminator controls were treated equally except that the enzyme was not added. The reaction was stopped by adding 5 mM EDTA, and was directly analyzed by an RNA blot after denaturation in standard MOPS loading buffer. All quantifications of RNA blots were done using the ImageQuant 5.2 software.

Luciferase assay

10^7 parasites were resuspended in 100 μl of lysis buffer (25 mM Tris–phosphate at pH 7.8, 2 mM dithiothreitol, 1% Triton X-100, 10% glycerol) and incubated at room temperature for 30 min, then transferred at −80°C for 2 h or overnight. After thawing, 20 μl of the parasite lysates was added to 96-well plates. One hundred microliters of luciferase assay buffer [20 mM tricine, 1.07 mM $(MgCO_3)4.Mg(OH)2.5\ H_2O$, 2.67 mM $MgSO_4$, 0.1 mM EDTA, 270 mM coenzyme A, 470 mM luciferin, 530 mM adenosine triphosphate, 33.3 mM DTT] was added to each well. Bioluminescence was measured using a Dynex MLX luminometer.

RESULTS

Quantitative analysis of the stage-specific mRNA regulation of the amastin mRNA

This study attempted to begin to elucidate mechanisms underlying mRNA degradation in *Leishmania* using the amastin mRNA as a model. The amastin gene encodes a putative surface antigen and is a member of a multi-gene family (49,50). What we refer to as amastin in this paper is the original gene that was first identified-LinJ34_v3.1030 (51). We previously demonstrated that most of the amastin mRNAs accumulate preferentially in amastigotes due to increased mRNA stability (49,51).

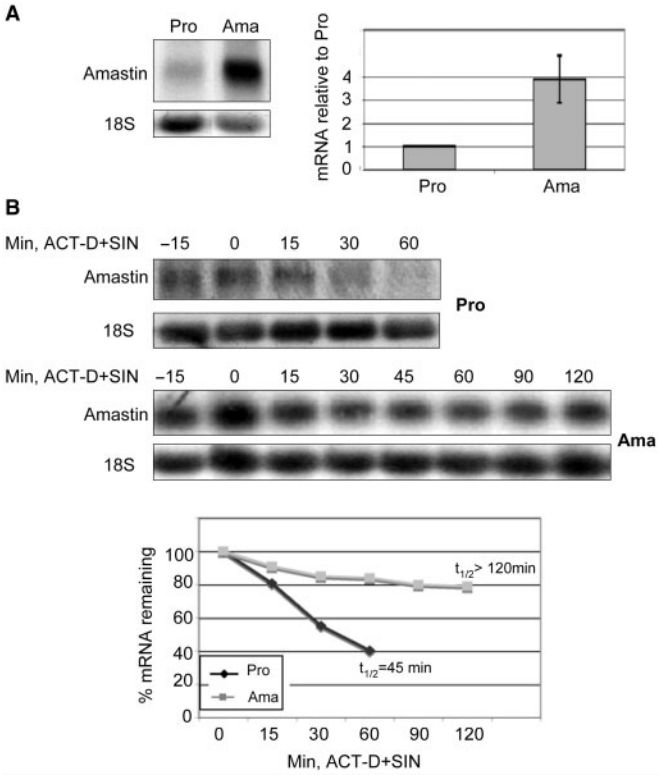

Figure 1. Endogenous amastin mRNA steady-state levels and decay kinetics. (**A**) RNA blot analysis of the amastin mRNA levels in promastigotes (Pro) and amastigotes (Ama). 18S was used as a loading control. Graphic representation of the data is shown in the right panel and values are relative to promastigotes. Blots were probed with one fragment which is complementary specifically to the last 300 bases of the amastin 3′UTR (probe 300, an average of three experiments), and another probe corresponding to the amastin-coding region (five experiments). (**B**) Decay kinetics of the amastin mRNA in promastigotes and amastigotes. 18S was used as a loading control. Blots were hybridized with probe 300. Note that the promastigote blot is over-exposed and comparison of steady-state levels with the amastigote blot is not advisable in this case. mRNA levels from different time points after transcriptional arrest with actinomycin-D (ACT-D) and inhibition of splicing with Sinefungin (SIN) were expressed relative to time 0 and data are representative of two experiments. '–15' denotes pre-treatment with SIN (including centrifugation time) before ACT-D is added at time 0. Graphic representations of the experiments are shown in the bottom panel. The absolute mRNA half-life values ($t_{1/2}$) in promastigotes and amastigotes are indicated. For mRNA half-life values derived from ACT-D treatment alone see Table 1.

We first wished to obtain a quantitative data on the amastin mRNA regulation by using an additional probe that is specific to the mRNA's 3′UTR, the last 300 bases (probe 300) to exclude possible cross-reactivity with other amastins. Overall the amastin mRNA is ∼3.9 more abundant in axenic amastigotes than in promastigotes-the developmental forms of the parasite that reside in the mammalian host and the insect vector, respectively (Figure 1A). The values obtained using the amastin coding sequence as a probe and the probe 300 are comparable and Figure 1A is representative of both. The decay kinetics of mRNAs was followed upon inhibition of

Table 1. mRNA half-lives for the endogenous amastin and reporter mRNAs analysed in this study

mRNA	mRNA half-lives (min)			
	ACT-D		ACT-D + SIN	
	Pro	Ama	Pro	Ama
Amastin	45 ± 20	>120	45 ± 15	>180
LUC-3′UTR	31.3 ± 19.6	82.5 ± 10.6	28 ± 15.5[a]	115 ± 10
LUC-3′UTRΔURE	>120	76 ± 1.4	63 ± 21.3[a]	137 ± 5

Decay rates for the endogenous amastin, *LUC-3′UTR* and *LUC-3′UTRΔURE* mRNAs in promastigotes (Pro) and axenic amastigotes (Ama) were determined after transcriptional inhibition using Actinomycin D (ACT-D) with or without splicing arrest using Sinefungin (SIN).

[a]Despite the variation of the absolute half-life values which are directly reflected in this Table, *LUC-3′UTRΔURE* mRNA was consistently more stable than *LUC-3′UTR* mRNA in promastigotes in each of the four independent experiments we carried out whereas no significant differences were observed between these two RNAs in amastigotes. Numerically, this parameter is reflected by the average of the relative differences (the half-life of *LUC-3′UTRΔURE* mRNA minus that of the *LUC-3′UTR* mRNA), which is 34 min ± an SD of 8 min.

de novo transcription using Actinomycin D and in some cases together with the arrest of splicing using Sinefungin. Sinefungin is assumed to prevent the splicing of pre-made pre-mRNAs by inhibiting the *de novo* methylation of the cap structure of the Spliced-Leader RNA (*SL-RNA*) and/or mRNA maturation from incomplete transcriptional inhibition. The combination of the two drugs was previously suggested to be important in drawing a more accurate representation of decay rates (11,30). Based on an analysis using the probe 300, the amastin mRNA decays with an overall half-life of ~40 min in promastigotes versus >120 min in amastigotes (Table 1, Figure 1B).

Stage-specific mRNA accumulation of the amastin mRNA is mediated through its 3′UTR

We asked if the stage-specific accumulation of the amastin mRNA is mediated through sequences in the 3′UTR, as is the case for most trypanosomatid mRNAs studied to date. For this and subsequent analysis, we made a bicistronic Neomycin-Luciferase (NEO-LUC) construct which contained the 3′UTR and the downstream intergenic region of the endogenous amastin locus directly after the LUC-coding sequence (Figure 2A). The construct also included additional intergenic and artificial sequences that allowed the proper maturation of the reporter LUC and the selectable marker NEO mRNAs. The NEO-LUC cassette is flanked by sequences that allowed the targeting of the construct into the Biopterin Transporter 1 (*BT1*) genomic locus by homologous recombination (data not shown). The protein encoded by the *BT1* gene is not required under culture conditions in biopterin-rich media but it is essential otherwise (52). The *BT1* locus is, therefore, used routinely for the integration of transgenic constructs, particularly when a physiologically relevant expression level is desirable. All the other sequences except the 3′UTR have been used routinely in several published [e.g. (33)] and unpublished reporter gene analysis and they do not affect RNA levels between promastigotes and amastigotes. Any difference in the LUC-amastin 3′UTR mRNA (*LUC-3′UTR*) levels should therefore be due to the amastin 3′UTR. Figure 2B shows that *LUC-3′UTR* mRNA is ~3.2-fold higher in amastigotes than in promastigotes, comparable with the regulation of the endogenous amastin mRNA (Figure 1A). mRNA decay analysis of the *LUC-3′UTR* showed that its half life is ~30 min in promastigotes and ~80 min in amastigotes (Table 1, Figure 3). In promastigotes, ~50–60% the *LUC-3′UTR* mRNA population are degraded with a half-life of ~10–15 min (Figure 3A and B). The rest of the population (40–50%) is degraded with a slower kinetics, the half-life being ~45 min (Figure 3A and B, data not shown). These results suggest that the stage specificity of the steady-state levels and degradation kinetics of the amastin mRNA are mediated mainly through sequences in its 3′UTR and that degradation is probably bi-phasic.

A U-rich ~100 bases region in the 3′UTR of the amastin mRNA contributes significantly to its stage-specific accumulation and its facilitated degradation in promastigotes

Next, we assessed whether the amastin mRNA regulation could be attributed to a distinct element in its 1.8 kb long 3′UTR. We have previously shown that the last 770 bases region of the amastin 3′UTR, in-and-by itself, does not account for stage-specific accumulation of the amastin mRNA (33). Sequence scanning of the rest of the 3′UTR revealed that it contains a ~100 bases long U-rich sequence (URE) (Figure 2A). Given the role of similar elements in the degradation of unstable mRNAs in other eukaryotes including *T. brucei* and *T. cruzi* [reviewed in (11,34)], we deleted this region in a construct which is otherwise identical to the LUC-3′UTR plasmid. The stable transfectant of this plasmid (LUC-3′UTRΔURE) was analyzed in parallel with that of the LUC-3′UTR. Copy number differences were ruled out by Southern blot analysis and comparison of *NEO* mRNA levels (data not shown). As shown in Figure 2B, the *LUC-3′UTRΔURE* mRNA steady-state levels are ~2.2-fold higher than that of *LUC-3′UTR* in promastigotes whereas no significant difference could be observed in amastigotes, suggesting that the URE accounts significantly for the stage-specific accumulation of the amastin mRNA. Decay analysis showed that the difference in the steady-state levels between *LUC-3′UTR* and *LUC-3′UTRΔURE* mRNA levels observed in promastigotes is accompanied by an overall increase in mRNA half-life from ~30 to >60 min (Figure 3A and B, Table 1). No significant changes could be detected in amastigotes (Figure 3C, Table 1). A more detailed comparison revealed that differences in degradation kinetics are more apparent in the initial phase (the first 15–30 min) than the later phase (Figure 3A and B). Luciferase activity levels generally followed the mRNA trends (Figure 2C, data not shown) and the URE-mediated mRNA degradation is, therefore, unlikely to be to due to differential translatability of the mRNA. Taken together, these results suggested that a significant part of the amastin mRNA degradation in promastigotes is

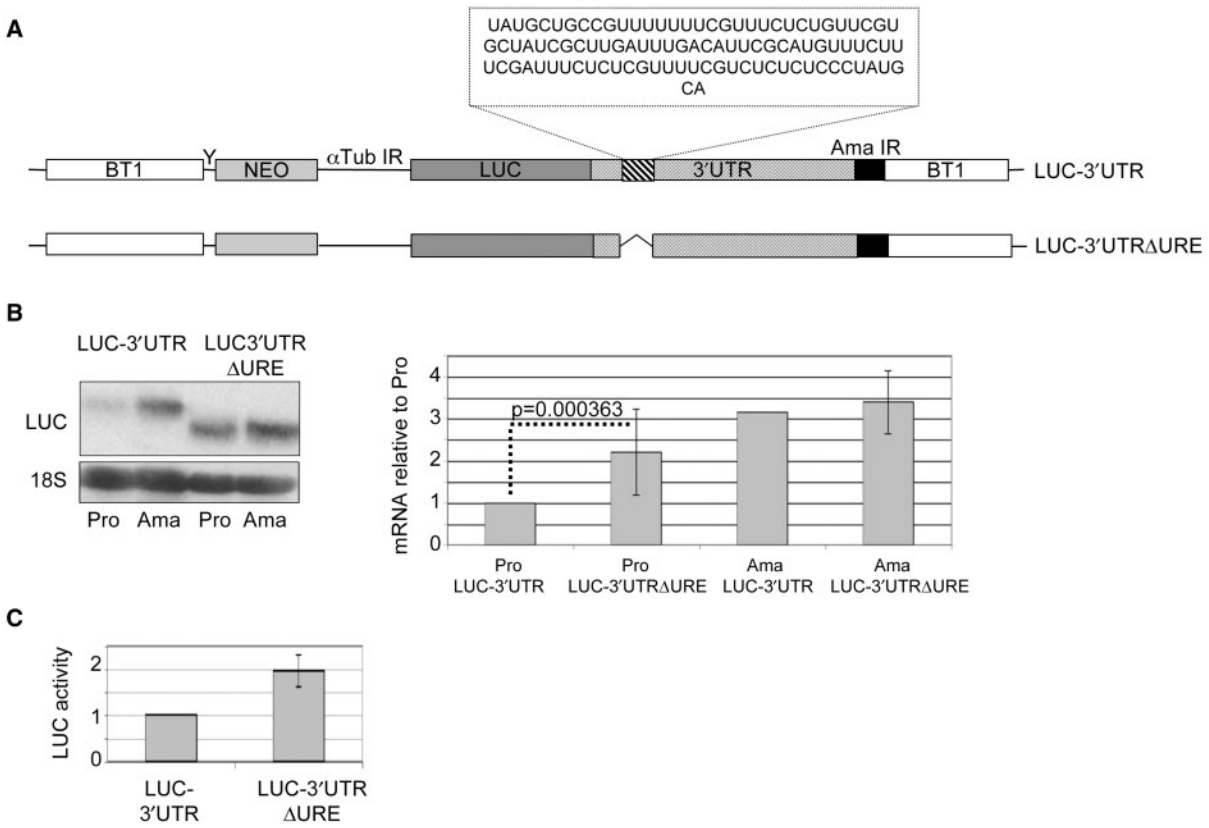

Figure 2. The use of reporter mRNAs to demonstrate the role of specific 3′UTR sequences in the stage-specific accumulation of the amastin mRNA. (**A**) Schematic representation of the reporter constructs, LUC-3′UTR and LUC-3′UTRΔURE. The exact sequence of the U-rich element (URE) that is deleted in LUC-3′UTRΔURE is indicated. The NEO-LUC bicistron is flanked with sequences that allow construct targeting to the endogenous *BT1* locus via homologous recombination. Y is a polypyrimidine stretch that allows 5′-end splicing of the Neomycin phosphotransferase (*NEO*) mRNA. αTub IR stands for the intergenic region of the alpha-tubulin gene and allows the 3′-end maturation of the *NEO* mRNA and the 5′-maturation of the Luciferase (*LUC*) mRNA. Ama IR denotes the intergenic region of the amastin gene, which allows the 3′-end maturation of the *LUC* mRNA. (**B**) RNA blot analysis of *LUC-3′UTR* and *LUC-3′UTRΔURE* mRNA levels in promastigotes (Pro) and amastigotes (Ama). 18S was used as a loading control. Graphic representation of the steady-state reporter mRNA levels is indicated in the right panel. Values are expressed relative to promastigote *LUC-3′UTR* mRNA levels. Data are derived from two to three experiments but 11 experiments for the *LUC-3′UTR* versus *LUC-3′UTRΔURE* comparisons in promastigotes. The *P*-value for the *LUC-3′UTR* versus *LUC-3′UTRΔURE* in promastigotes is shown and was calculated using Excel's Type 3 two-tailed *T*-test. (**C**) Luciferase activity in promastigotes. Luciferase (LUC) protein levels were inferred by measuring LUC enzymatic activity. Data are derived from three experiments.

URE-mediated and that this probably occurs during the initiation phase of the degradation.

Differential degradation of the amastin mRNA in promastigotes seems to be initiated via deadenylation-independent mechanisms

mRNA degradation in eukaryotes is typically initiated and modulated via differential deadenylation [reviewed in (13)]. Thus, we asked if the promastigote-specific degradation of the amastin mRNA is due to rapid deadenylation. The endogenous amastin or *LUC-3′UTR* mRNAs are relatively long (~2.6 and ~3.5 kb, respectively) and changes in mRNA sizes due to deadenylation in ordinary RNA blot analysis would be difficult to visualize. We, therefore, like in many other previous studies by others [e.g. (24)], exploited the DNA–RNA hybrid-dependent ribonuclease activity of RNase H to cleave these RNAs at specific sites and generate shorter 3′-end fragments. This was achieved by incubating RNA samples from several time points after ACT-D ± SIN treatments with RNase H in the presence of anti-sense oligonucleotide targeted to a region of ~300 bases from the end of the amastin 3′UTR (Figure 4A). Oligo dT was added in some samples so that the poly(A) tail could be cleaved off and the resulting fragment served as a marker for a ~100% deadenylated mRNA species. This analysis in promastigotes showed that the poly(A) tail of the *LUC-3′UTR* mRNA is still intact (relative to time 0) long after a significant part of the mRNA body has been degraded (Figure 4B, left panel). In contrast, a significant deadenylation clearly precedes the degradation of the mRNA in amastigotes (Figure 4B, right panel). Interestingly, the deadenylation pattern of the relatively more stable *LUC-3′UTRΔURE* mRNA was not different between promastigotes (Figure 4B, middle panel) and amastigotes (data not shown) and it remarkably resembles that of *LUC-3′UTR* in amastigotes (Figure 4B, right panel). Noteworthy, a minor population of the *LUC-3′UTR* mRNA in promastigotes appears to be deadenylated at

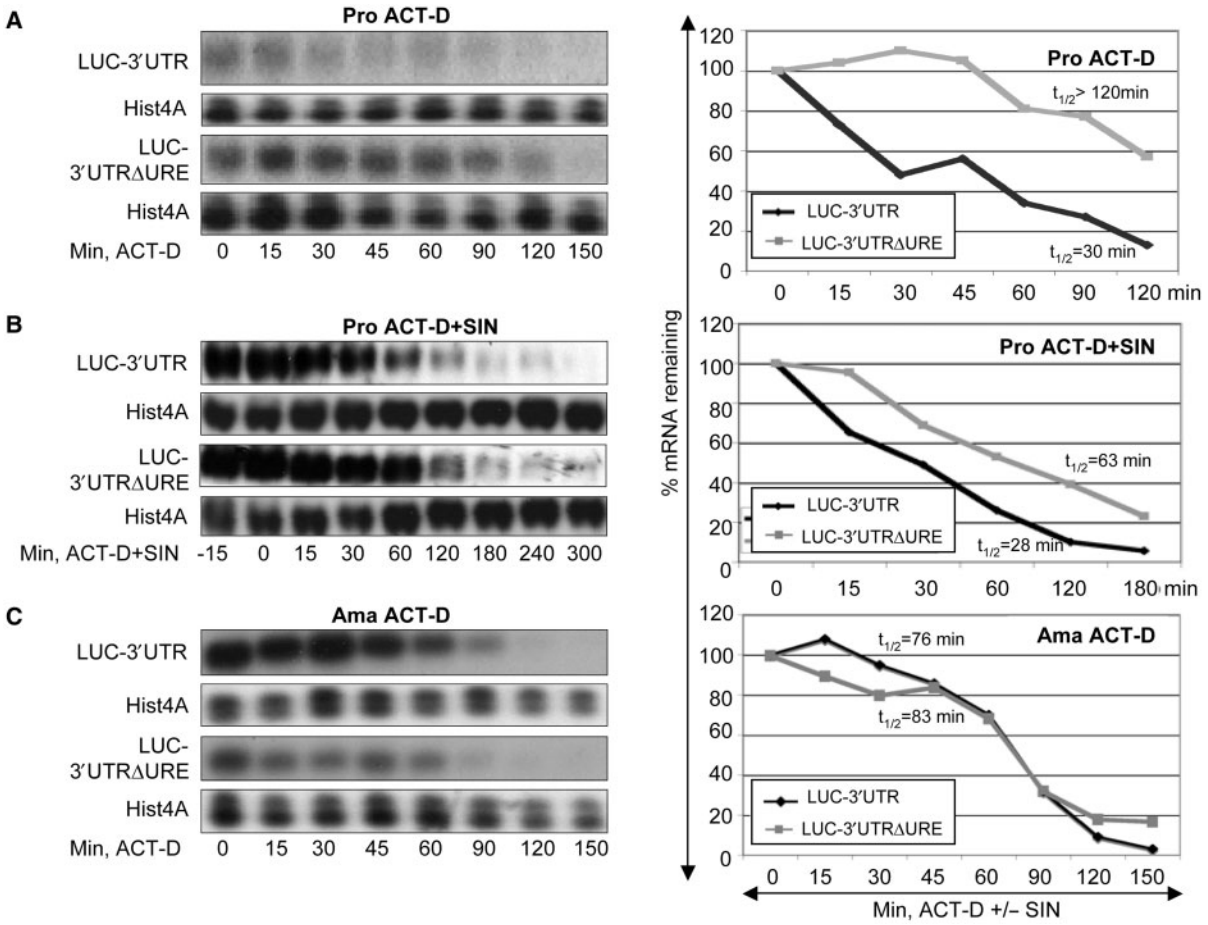

Figure 3. Decay kinetics of reporter mRNAs. mRNA decay rate was followed after inhibition of transcription alone with Actinomycin D (ACT-D) for *LUC-3′UTR* versus *LUC-3′UTRΔURE* in promastigotes (Pro) (**A**), ACT-D plus Sinefungin (SIN) for *LUC-3′UTR* versus *LUC-3′UTRΔURE* in Promastigotes (**B**) and ACT-D alone for *LUC-3′UTR* versus *LUC-3′UTRΔURE* in amastigotes (Ama) (**C**). '–15' time point in (B) represents a pre-treatment with SIN (including centrifugation time) before the addition of ACT-D at time 0. Histone 4A (Hist4A) was used as a loading control. Graphic representations of mRNA decay rates are indicated on the right panels where mRNA levels from different time points (after ACT-D with or without SIN treatments) were expressed relative to time 0. Data are derived from two experiments for the amastigote data and four experiments for the promastigote data. The absolute mRNA half-life values ($t_{1/2}$) are indicated. See Table 1 for the entire complement of mRNA half-lives calculated in this study and their corresponding standard errors.

later time points (the last lanes in Figure 4B, left panel and 4C) and is probably coincident with the second and slower phase of the mRNA degradation (Figure 3A and B).

We carried out a similar analysis for the endogenous amastin mRNA both in promastigotes and amastigotes. In order to detect the deadenylation pattern of the endogenous amastin mRNA in promastigotes (expression of the amastin mRNA is much higher in amastigotes compared to promastigotes), we had to increase the sensitivity of the assay and to expose the Northern blots much longer. This analysis shows that consistent with the reporter mRNA results described earlier (Figure 4B, left panel), the amastin mRNA in promastigotes—in contrast to the same mRNA in amastigotes—is degraded without detectable deadenylation (Figure 5A and C upper panel). We next wanted to assess the deadenylation profile of the amastin mRNA during differentiation. To induce differentiation *in vitro*, we subject amastigotes grown at 37°C and pH 5.8 to promastigote conditions (25°C and pH 7.0) of growth. Approximately 5 h following the switch from amastigote to promastigote conditions, a significant decrease in amastin mRNA levels could be observed (Figure 5B). Interestingly, under these conditions, the deadenylation pattern of the endogenous amastin mRNA (Figure 5C lower panel) was comparable to that seen using adapted promastigote cultures (Figure 5A). Overall, these results suggest that the initial phase of the degradation of the amastin mRNA in promastigotes *per se* is likely to be deadenylation-independent and that the stage-specific regulation of the amastin mRNA is unlikely to be a function of differential deadenylation rate.

Is decapping the rate-limiting step for the promastigote-specific degradation of the amastin mRNA?

Deadenylation-independent mechanisms of mRNA degradation are rare in eukaryotes and are mainly initiated via an endonuclease or deadenylation-independent decapping activities. A role for a decapping mechanism is usually demonstrated via genetic or RNA interference (RNAi) approaches. However, no clear homologue of a decapping

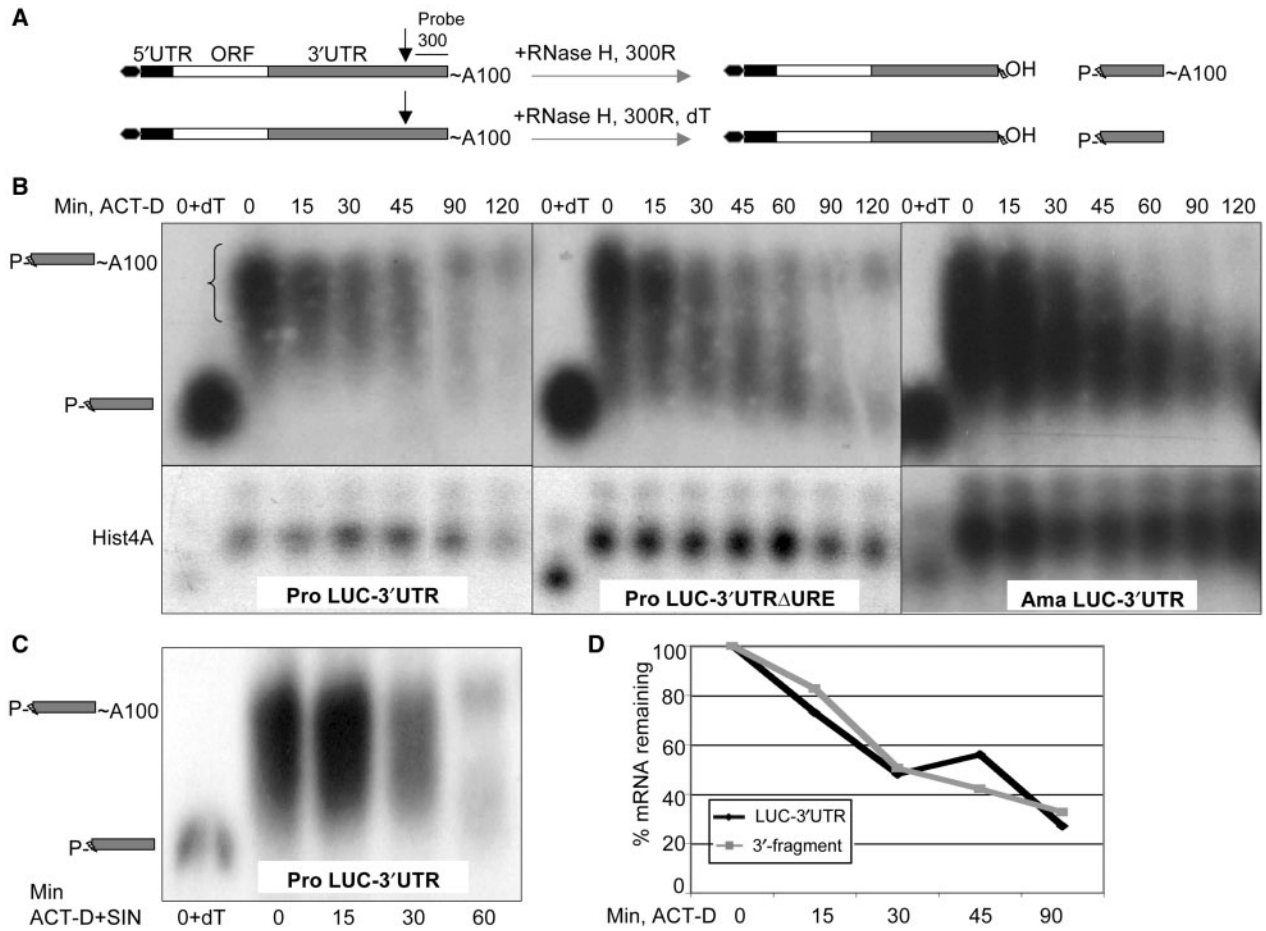

Figure 4. Determination of poly(A) tail status during reporter mRNA decay. (**A**) Schematic representation of the deadenylation assay. RNase-H digests DNA/RNA hybrid. In this case the DNA is an oligonucleotide (300R), which is reverse complementary to a region of ~300 bases upstream of the poly(A) tail of the reporter mRNA. The presence of oligo dT in the reaction allows the trimming of the poly(A) tails (see later). The vertical darker arrows indicate the sequence to which the oligonucleotide was targeted into. The last 300 bases of the 3′UTR is underlined and is where the probe for the RNA blots was targeted. (**B**) Deadenylation of reporter mRNAs in promastigotes (Pro) and amastigotes (Ama). RNA samples were collected from different time points after treatment with ACT-D and subjected to RNase-H treatment. 3′ fragments were analysed by RNA blot. At time 0, RNA samples were also treated with RNase-H digestion in the presence of oligo dT (in addition to the specific oligonucleotide) to generate poly(A) minus 3′-end markers ('0 + dT' lanes). Hist 4A is used as a loading control. (**C**) As in (B) but RNA was derived from ACT-D and SIN treatment of *LUC-3′UTR* promastigotes. Data are representative of three experiments. (**D**) Quantitative representation of the decay rate of *LUC-3′UTR* polyadenylated 3′-end fragments in promastigotes (B, left panel) is compared to that of the full-length *LUC-3′UTR* mRNA in promastigotes (Figure 3A). The lateral bracket indicated in Figure 4B left panel shows the portion of the gel used for quantification of the largely poly(A)+ 3′-end fragments. Note that the full-length *LUC-3′UTR* mRNA used for this quantification was probed by the luciferase coding sequence, which is ~1.8 kb upstream of the polyadenylation site while the 3′-end products of the RNase H were probed by the last 300 terminal sequence of the 3′-end.

enzyme could so far be identified in the genomes of trypanosomatids. We, therefore, resorted in this study into an indirect assessment of the decapping rate of the *LUC-3′UTR* mRNA versus the *LUC-3′UTRΔURE* mRNA in promastigotes. To do this, we took advantage of the commercially available 5′-phosphate-dependent riboexonuclease, Terminator, which has so far been used mainly to enrich mRNA preparation as the enzyme degrades all uncapped RNAs (e.g. decapped mRNAs, rRNAs, tRNAs) while capped mRNAs are protected. A recent study has made use of the enzyme to qualitatively access the cap status of a deadenylated intermediate of the *hsp70* mRNA (53). Here, we anticipated that relative mRNA decapping rates could quantitatively be inferred by comparison of Terminator treated versus untreated RNA samples derived from various time points after transcriptional arrest. For this assay, uncapped rRNAs that are cleaved by the enzyme served as positive controls (with 50–80% efficiency in our case). Histone 4A (*Hist4A*) mRNA is very stable within the time points used in the assay and therefore served as a negative control and indicated that the enzyme is highly specific (Figure 6A). Tube-to-tube variations in the efficiency of the Terminator activity were corrected with the levels of 18S RNA after loading normalization with the *Hist4A* mRNA (Figure 6A). Values from Terminator-treated samples were then divided by those from Terminator-untreated samples. The resulting numbers for each of the various time points after ACT-D treatment were expressed as a function of time 0. Such analysis indicated that there is no significant difference between the percentage of capped *LUC-3′UTR* and *LUC-3′UTRΔURE* mRNAs at various

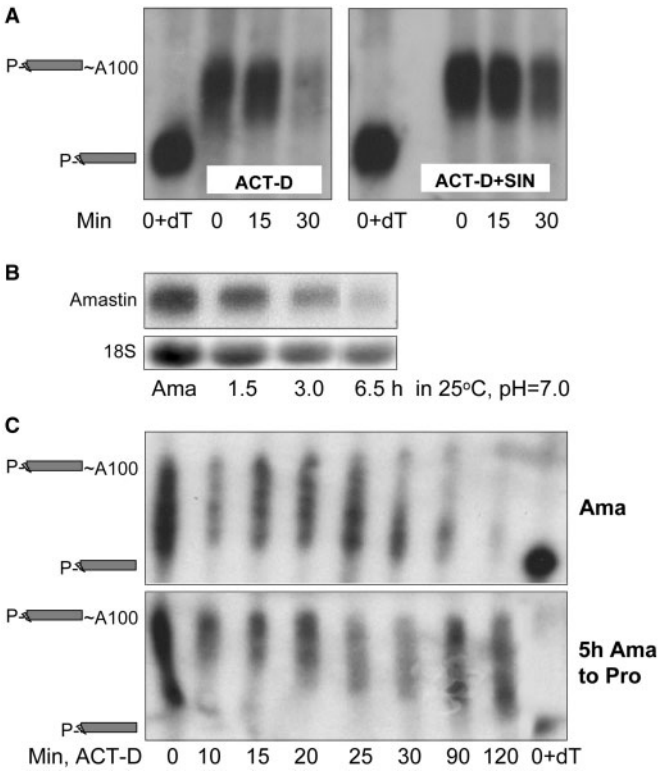

Figure 5. Deadenylation analysis of the endogenous amastin mRNA. (**A**) RNase H-RNA blot deadenylation assay for assessing deadenylation of the endogenous amastin mRNA in promastigotes. RNA samples were collected at 0, 15 and 30 min (half-life of the endogenous mRNA in promastigotes, see Figure 1B) following transcriptional arrest with Actinomycin-D (ACT-D) (left panel) and treatment with ACT-D plus Sinefungin (SIN) to inhibit splicing (right panel) and subjected to RNase-H treatment as detailed in Figure 4 and under 'Materials and Methods' section. (**B**) Time-point analysis of the amastin mRNA during a switch from axenic amastigote (Ama) (pH 5.8, 37°C) to promastigote (Pro) (pH 7.0, 25°C) conditions. Blots were probed with the probe 300 fragment. (**C**) RNase H-RNA blot deadenylation assay. The 5 h post-switch was selected based on the data presented in (B), a time point where a detectable decrease in mRNA level was observed and yet not down to an extent below the detection limit of the deadenylation assay. RNA samples were run on 5% polyacrylamide gels. Other methodological details for the deadenylation analysis are as in Figure 4. The data are representative of two experiments.

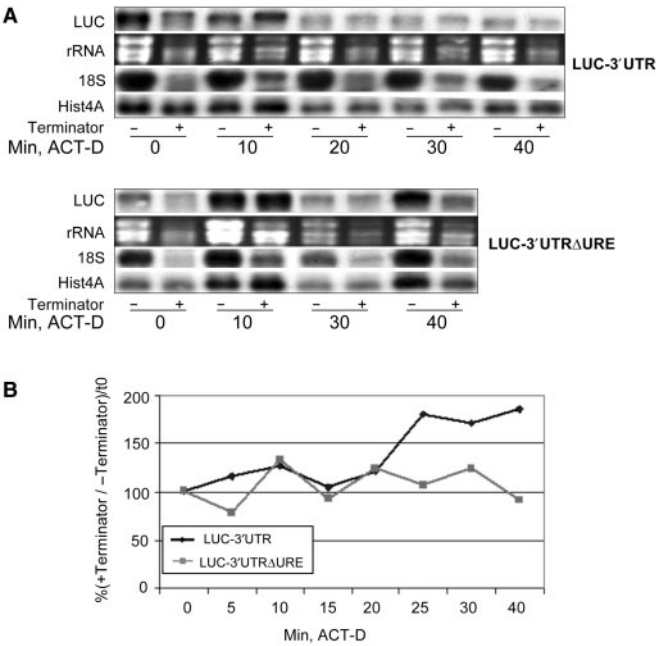

Figure 6. Indirect measurement of decapping rates. (**A**) RNA samples were derived from LUC-3′UTR and LUC-3′UTRΔURE lines treated with actinomycin-D (ACT-D) for different time points. An equal volume of RNA was separated into two different tubes. One set of the tubes contained the reaction mix containing the Terminator enzyme (+ lanes) and the other contained the same mix but without the enzyme (– lanes). Both Terminator – and + reactions were incubated for 1–1.5 h according to manufacturer's instructions (Epicentre Biotechnologies). Data are representative of two experiments. Similar results were obtained in two other experiments involving ACT-D and SIN (data not shown). 18S RNA signals were used to control for tube-to-tube variation of Terminator degradation efficiency after normalization of loading with histone 4A (*Hist4A*) mRNA. (**B**) Graphic representation of the ratio of + Terminator signals to – Terminator signals relative to time 0.

time points after transcriptional arrest (relative to time 0) (Figure 6B). These results, within the limits of the assay employed, suggested that no detectable difference in decapping rate can account for the URE-mediated facilitated degradation of the amastin mRNA in promastigotes.

DISCUSSION

In this study, we began a series of experiments aimed at dissecting the mechanisms of mRNA degradation responsible for the expression of stage-specific mRNAs in *Leishmania*. Specifically, we studied the degradation of the amastin mRNA, which was previously shown to be more abundant in amastigotes than in promastigotes (51). Further interest in undertaking this study stems from the observations that the amastin gene encodes a putative surface protein and is a member of multi-gene family with an expected role in the biology and/or pathobiology of the parasite (49,50).

In common with a number of other previously studied mRNAs, the stage-specific amastin mRNA is regulated via sequences in its 3′UTR at the level of mRNA stability. Sequence analysis of its 3′UTR revealed the presence of a ~100 bases long U-rich sequence (URE) and our reporter mRNA analysis showed that this element contributes significantly to the stage-specific accumulation and degradation of the amastin mRNA. A similar role of UREs was previously shown for *T. brucei* and *T. cruzi* mRNAs [reviewed in (11,34)], suggesting that this mechanism is probably conserved in trypanosomatids. Noteworthy, the designation of this element as a URE, and its reference relative to elements in other eukaryotes, is solely based on the relatively high (50%) U-content of the region. Also, the specific regulatory region within the element, if distinct at all, might not necessarily be as U-rich.

The URE does not seem to account for all of the stage-specific regulation of the amastin mRNA. If any, the rest of the amastin mRNA regulation might be explained by other elements in its 1.8 kb 3′UTR. The 3′UTR of the amastin mRNA contains a sequence related to the

Leishmania specific SIDER1 retroelements (31). We have previously shown that the amastin SIDER1 alone does not alter reporter RNA levels (33). However, the possibility that it might have a context dependent function, perhaps in synergy with the URE, remains to be tested.

mRNA decay analysis of the amastin mRNA revealed a remarkable resemblance of degradation kinetics with that of unstable mRNAs in *T. brucei*. Unlike the degradation of the stable mRNAs, at least the initial phase of the degradation of unstable URE-containing mRNAs appears to be deadenylation-independent (24,29). At least at first glance, an alternative interpretation of the deadenylation analysis we employed in this study can be associated with the possibility that deadenylated species of the endogenous amastin or *LUC-3′UTR* mRNAs in promastigotes might be degraded too fast to be detectable. Our data do not rule out the singular possibility that deadenylated amastin mRNA species might be degraded faster in promastigotes. However, whether the differential degradation of the amastin mRNA is mediated through and/or preceded by undetectable deadenylation is altogether a different question. Several indications seem to go against this possibility. First, there are no appreciable levels of deadenylated species at time 0 and at early time points following actinomycin D treatment. Secondly, deadenylated species are actually detectable in the later time points (Figure 4B left panel and Figure 4C). Thirdly, as mRNAs get deadenylated, there must be a proportional decrease of the poly(A) plus mRNAs. This would imply that the remaining polyadenylated portion of the 3′-end fragments should disappear faster relative to the full-length mRNA. However, our results did not indicate that this is the case (Figures 3 and 4). In fact, the decay kinetics of the non-deadenylated 3′-end fragments was not distinguishable from those of the full-length, RNase-H-untreated mRNAs (Figure 4D). Fourthly, we did not observe detectable differences when we compared degradation from the 5′- and 3′-ends in RNase H-RNA blots using an oligonucleotide that allowed cutting at ~800 bases upstream of the 3′-end and subsequent detection with region-specific probes (see Supplementary Data in Figure S1). Indeed, RNAi-mediated depletion of a homologue of a yeast deadenylase in *T. brucei* has minimal effects on the degradation kinetics of unstable mRNAs (including URE-mRNAs) while that of moderately and highly stable mRNAs is clearly altered (personal communication by Dr Clayton, ZMBH, Germany). These observations collectively compelled us to conclude that the URE-mediated promastigote-specific degradation of the amastin mRNA is deadenylation-independent. It is, therefore, tempting to suggest that the likely possibility that deadenylated species might be degraded faster in promastigotes can instead be viewed as further evidence to our conclusion; namely that URE amastin mRNAs are degraded faster in promastigotes regardless of whether they contain poly(A) or not (i.e. degradation is independent of deadenylation status).

Significant levels of deadenylated species are detectable at steady-state in both stages of the parasite. This is a surprising observation because deadenylated mRNAs are considered to be unstable. Interestingly, a recent global analysis of poly(A) length of mammalian mRNAs has revealed a surprisingly high proportion of the mRNAs (~25%) having oligoadenylated species with only <30 length of poly(A) (54). Even a more surprising finding of the study by Meijer *et al*. is that some stable mRNAs fall among these mRNAs. For example, 25% of the beta-actin mRNA, an mRNA known to be very stable, contained a short poly(A) tail. These observations collectively challenge the current notion that deadenylated mRNA species are unstable. A related observation in this study is that a higher proportion of deadenylated and oligoadenylated species are detected for stable mRNAs (the amastin or *LUC-3′UTR* mRNAs in amastigotes and the *LUC-3′UTRΔURE* mRNA in both stages) than unstable mRNAs (the amastin and *LUC-3′UTR* mRNAs in promastigotes). This can be because the deadenylated species are degraded faster in promastigotes. Alternatively, this can be viewed as an indication for the possibility that the URE-mediated regulation of the amastin mRNA is not only deadenylation-independent but also polyadenylation-dependent. In other words, the poly(A) tail might have a destabilizing role rather than a stabilizing one. In bacteria, poly(A) tail serves as a 'holding toe' for 3′-exonucleases thereby facilitating degradation (55). However, this is not the case for almost all functional eukaryotic mRNAs studied so far. The few cases where poly(A) tail has a destabilizing function in eukaryotes fall within the realms of nuclear RNA degradation of certain pre-mRNAs and/or aberrant mRNAs as part of quality-control mechanisms (56–58).

Mechanisms of deadenylation-independent mRNA degradation, albeit rare, include deadenylation-independent decapping mechanisms such as the one associated with at least one pathway of the non-sense-mediated decay (59,60). Unfortunately, no clear homologue to any of the decapping enzymes from other eukaryotes has so far been identified in the genomes of trypanosomatids even though *in vitro* decapping activity was biochemically detected in a related species (23). In this study, we attempted to indirectly compare decapping rates by taking advantage of a 5′-phosphate-dependent enzyme, Terminator. This analysis did not show a significant difference between *LUC-3′UTR* and *LUC-3′UTRΔURE* mRNAs in promastigotes suggesting the differential mRNA degradation is unlikely to be a function of an altered decapping rate. We, therefore, favor the scenario that an endonuclease-mediated cleavage might be the rate-limiting step, a well-studied example of which can be found in the degradation of the mammalian alpha-globin mRNA [reviewed in (61)]. Alternatively, a novel pathway might be awaiting a discovery.

Our current model of the amastin mRNA degradation based on this study, and in analogy with the situation in *T. brucei*, is that two mechanisms are likely to be involved: one that appears to be deadenylation- and decapping-independent, URE-mediated rapid degradation that is developmentally regulated, and the other is constitutive, which is likely to be slower and deadenylation-dependent (Figure 7). This study is the first not only in reporting a URE-mediated degradation in *Leishmania* but also in

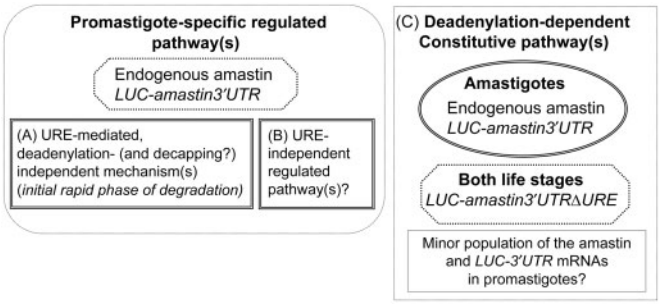

Figure 7. A proposed model for the stage-specific mRNA degradation of the amastin mRNA. A significant part of the promastigote-specific facilitated degradation of the amastin mRNA (and the *LUC-3′UTR* mRNA) is URE-dependent, is mostly deadenylation-independent and probably decapping-independent (**A**). An additional unknown mechanism that is URE-independent (**B**) might be involved as well because deletion of the URE did not account for all of the stage-specific mRNA regulation at the steady-state levels as indicated in Figure 2. A constitutive deadenylation-dependent pathway (**C**) is responsible for the decay of more stable mRNAs *(LUC-3′UTRΔURE* in both developmental forms, and the amastin and *LUC-3′UTR* mRNAs in amastigotes). A minor sub-population of the amastin and *LUC-3′UTR* mRNAs in promastigotes is probably degraded via a deadenylation-dependent constitutive pathway.

attempting to draw the mechanistic basis of differential mRNA degradation in this parasite. The extent to which URE-mediated degradation differs from mammalian ARE-mediated mRNA instability and whether there are species-specific aspects of this mechanism among trypanosomatids remain to be determined.

SUPPLEMENTARY DATA

Supplementary Data are available at NAR Online.

ACKNOWLEDGEMENTS

This work was supported by the Canadian Institutes of Health Research (CIHR) MOP-12182 operating grant to B.P. S.H. is supported by a postdoctoral fellowship from the CIHR. A.D. is a recipient of a fellowship from the CIHR STP-53924 Strategic Training Program. We thank all Papadopoulou lab members for discussions, and Annie Rochette for sharing some unpublished data. We are also indebted to Dr Christine Clayton (ZMBH, University of Heidelberg) for critical reading of the manuscript and for communicating unpublished data. Funding to pay the Open Access publication charges for this article was provided by the CIHR MOP-12182 grant.

Conflict of interest statement. None declared.

REFERENCES

1. Cohen-Freue,G., Holzer,T.R., Forney,J.D. and McMaster,W.R. (2007) Global gene expression in Leishmania. *Int. J. Parasitol.*, **37**, 1077–1086.
2. Brems,S., Guilbride,D.L., Gundlesdodjir-Planck,D., Busold,C., Luu,V.D., Schanne,M., Hoheisel,J. and Clayton,C. (2005) The transcriptomes of Trypanosoma brucei Lister 427 and TREU927 bloodstream and procyclic trypomastigotes. *Mol. Biochem. Parasitol.*, **139**, 163–172.
3. Minning,T.A., Bua,J., Garcia,G.A., McGraw,R.A. and Tarleton,R.L. (2003) Microarray profiling of gene expression during trypomastigote to amastigote transition in Trypanosoma cruzi. *Mol. Biochem. Parasitol.*, **131**, 55–64.
4. Atwood,J.A.,3rd, Weatherly,D.B., Minning,T.A., Bundy,B., Cavola,C., Opperdoes,F.R., Orlando,R. and Tarleton,R.L. (2005) The Trypanosoma cruzi proteome. *Science*, **309**, 473–476.
5. Berriman,M., Ghedin,E., Hertz-Fowler,C., Blandin,G., Renauld,H., Bartholomeu,D.C., Lennard,N.J., Caler,E., Hamlin,N.E. *et al.* (2005) The genome of the African trypanosome Trypanosoma brucei. *Science*, **309**, 416–422.
6. El-Sayed,N.M., Myler,P.J., Blandin,G., Berriman,M., Crabtree,J., Aggarwal,G., Caler,E., Renauld,H., Worthey,E.A. *et al.* (2005) Comparative genomics of trypanosomatid parasitic protozoa. *Science*, **309**, 404–409.
7. Ivens,A.C., Peacock,C.S., Worthey,E.A., Murphy,L., Aggarwal,G., Berriman,M., Sisk,E., Rajandream,M.A., Adlem,E. *et al.* (2005) The genome of the kinetoplastid parasite, Leishmania major. *Science*, **309**, 436–442.
8. Liang,X.H., Haritan,A., Uliel,S. and Michaeli,S. (2003) trans and cis splicing in trypanosomatids: mechanism, factors, and regulation. *Eukaryot. Cell*, **2**, 830–840.
9. Martinez-Calvillo,S., Yan,S., Nguyen,D., Fox,M., Stuart,K. and Myler,P.J. (2003) Transcription of Leishmania major Friedlin chromosome 1 initiates in both directions within a single region. *Mol. Cell*, **11**, 1291–1299.
10. Martinez-Calvillo,S., Nguyen,D., Stuart,K. and Myler,P.J. (2004) Transcription initiation and termination on Leishmania major chromosome 3. *Eukaryot. Cell*, **3**, 506–517.
11. Clayton,C. and Shapira,M. (2007) Post-transcriptional regulation of gene expression in trypanosomes and leishmanias. *Mol. Biochem. Parasitol.*, **156**, 93–101.
12. Haile,S. and Papadopoulou,B. (2007) Developmental regulation gene expression in trypanosomatid parasitic protozoa. *Curr. Opin. Microbiol.*, **10**, 569–577.
13. Parker,R. and Song,H. (2004) The enzymes and control of eukaryotic mRNA turnover. *Nat. Struct. Mol. Biol.*, **11**, 121–127.
14. Mitchell,P. and Tollervey,D. (2000) mRNA stability in eukaryotes. *Curr. Opin. Genet. Dev.*, **10**, 193–198.
15. Heyer,W.D., Johnson,A.W., Reinhart,U. and Kolodner,R.D. (1995) Regulation and intracellular localization of Saccharomyces cerevisiae strand exchange protein 1 (Sep1/Xrn1/Kem1), a multifunctional exonuclease. *Mol. Cell. Biol.*, **15**, 2728–2736.
16. Johnson,A.W. (1997) Rat1p and Xrn1p are functionally interchangeable exoribonucleases that are restricted to and required in the nucleus and cytoplasm, respectively. *Mol. Cell. Biol.*, **17**, 6122–6130.
17. Amberg,D.C., Goldstein,A.L. and Cole,C.N. (1992) Isolation and characterization of RAT1: an essential gene of Saccharomyces cerevisiae required for the efficient nucleocytoplasmic trafficking of mRNA. *Genes Dev.*, **6**, 1173–1189.
18. Allmang,C., Kufel,J., Chanfreau,G., Mitchell,P., Petfalski,E. and Tollervey,D. (1999) Functions of the exosome in rRNA, snoRNA and snRNA synthesis. *Embo J.*, **18**, 5399–5410.
19. Bousquet-Antonelli,C., Presutti,C. and Tollervey,D. (2000) Identification of a regulated pathway for nuclear pre-mRNA turnover. *Cell*, **102**, 765–775.
20. Chen,C.Y., Gherzi,R., Ong,S.E., Chan,E.L., Raijmakers,R., Pruijn,G.J., Stoecklin,G., Moroni,C., Mann,M. *et al.* (2001) AU binding proteins recruit the exosome to degrade ARE-containing mRNAs. *Cell*, **107**, 451–464.
21. Mukherjee,D., Gao,M., O'Connor,J.P., Raijmakers,R., Pruijn,G., Lutz,C.S. and Wilusz,J. (2002) The mammalian exosome mediates the efficient degradation of mRNAs that contain AU-rich elements. *Embo J.*, **21**, 165–174.
22. Stoecklin,G., Mayo,T. and Anderson,P. (2006) ARE-mRNA degradation requires the 5′-3′ decay pathway. *EMBO Rep.*, **7**, 72–77.
23. Milone,J., Wilusz,J. and Bellofatto,V. (2002) Identification of mRNA decapping activities and an ARE-regulated 3′ to 5′ exonuclease activity in trypanosome extracts. *Nucleic Acids Res.*, **30**, 4040–4050.

24. Irmer,H. and Clayton,C. (2001) Degradation of the unstable EP1 mRNA in Trypanosoma brucei involves initial destruction of the 3′-untranslated region. *Nucleic Acids Res.*, **29**, 4707–4715.
25. Estevez,A.M., Kempf,T. and Clayton,C. (2001) The exosome of Trypanosoma brucei. *Embo J.*, **20**, 3831–3839.
26. Estevez,A.M., Lehner,B., Sanderson,C.M., Ruppert,T. and Clayton,C. (2003) The roles of intersubunit interactions in exosome stability. *J. Biol. Chem.*, **278**, 34943–34951.
27. Haile,S., Cristodero,M., Clayton,C. and Estevez,A.M. (2007) The subcellular localisation of trypanosome RRP6 and its association with the exosome. *Mol. Biochem. Parasitol.*, **151**, 52–58.
28. Li,C.H., Irmer,H., Gudjonsdottir-Planck,D., Freese,S., Salm,H., Haile,S., Estevez,A.M. and Clayton,C. (2006) Roles of a Trypanosoma brucei 5′->3′ exoribonuclease homolog in mRNA degradation. *RNA*, **12**, 2171–2186.
29. Haile,S., Estevez,A.M. and Clayton,C. (2003) A role for the exosome in the in vivo degradation of unstable mRNAs. *RNA*, **9**, 1491–1501.
30. Colasante,C., Robles,A., Li,C.H., Schwede,A., Benz,C., Voncken,F., Guilbride,D.L. and Clayton,C. (2007) Regulated expression of glycosomal phosphoglycerate kinase in Trypanosoma brucei. *Mol. Biochem. Parasitol.*, **151**, 193–204.
31. Bringaud,F., Muller,M., Cerqueira,G.C., Smith,M., Rochette,A., El-Sayed,N.M., Papadopoulou,B. and Ghedin,E. (2007) Members of a large retroposon family are determinants of post-transcriptional gene expression in *Leishmania*. *PLoS Pathog.*, **3**(9), 1291–1307.
32. Boucher,N., Wu,Y., Dumas,C., Dubé,M., Sereno,D., Breton,M. and Papadopoulou,B. (2002) A common mechanism of stage-regulated gene expression in Leishmania mediated by a conserved 3′-untranslated region element. *J. Biol. Chem.*, **277**, 19511–19520.
33. McNicoll,F., Muller,M., Cloutier,S., Boilard,N., Rochette,A., Dube,M. and Papadopoulou,B. (2005) Distinct 3′-untranslated region elements regulate stage-specific mRNA accumulation and translation in Leishmania. *J. Biol. Chem.*, **280**, 35238–35246.
34. D'Orso,I., De Gaudenzi,J.G. and Frasch,A.C. (2003) RNA-binding proteins and mRNA turnover in trypanosomes. *Trends Parasitol.*, **19**, 151–155.
35. Drozdz,M. and Clayton,C. (1999) Structure of a regulatory 3′ untranslated region from Trypanosoma brucei. *RNA*, **5**, 1632–1644.
36. Hotz,H.R., Hartmann,C., Huober,K., Hug,M. and Clayton,C. (1997) Mechanisms of developmental regulation in Trypanosoma brucei: a polypyrimidine tract in the 3′-untranslated region of a surface protein mRNA affects RNA abundance and translation. *Nucleic Acids Res.*, **25**, 3017–3026.
37. Di Noia,J.M., D'Orso,I., Sanchez,D.O. and Frasch,A.C. (2000) AU-rich elements in the 3′-untranslated region of a new mucin-type gene family of Trypanosoma cruzi confers mRNA instability and modulates translation efficiency. *J. Biol. Chem.*, **275**, 10218–10227.
38. D'Orso,I. and Frasch,A.C. (2001) Functionally different AU- and G-rich cis-elements confer developmentally regulated mRNA stability in Trypanosoma cruzi by interaction with specific RNA-binding proteins. *J. Biol. Chem.*, **276**, 15783–15793.
39. Quijada,L., Guerra-Giraldez,C., Drozdz,M., Hartmann,C., Irmer,H., Ben-Dov,C., Cristodero,M., Ding,M. and Clayton,C. (2002) Expression of the human RNA-binding protein HuR in Trypanosoma brucei increases the abundance of mRNAs containing AU-rich regulatory elements. *Nucleic Acids Res.*, **30**, 4414–4424.
40. Mayho,M., Fenn,K., Craddy,P., Crosthwaite,S. and Matthews,K. (2006) Post-transcriptional control of nuclear-encoded cytochrome oxidase subunits in Trypanosoma brucei: evidence for genome-wide conservation of life-cycle stage-specific regulatory elements. *Nucleic Acids Res.*, **34**, 5312–5324.
41. Chen,C.Y., Xu,N. and Shyu,A.B. (1995) mRNA decay mediated by two distinct AU-rich elements from c-fos and granulocyte-macrophage colony-stimulating factor transcripts: different deadenylation kinetics and uncoupling from translation. *Mol. Cell. Biol.*, **15**, 5777–5788.
42. D'Orso,I. and Frasch,A.C. (2001) TcUBP-1, a developmentally regulated U-rich RNA-binding protein involved in selective mRNA destabilization in trypanosomes. *J. Biol. Chem.*, **276**, 34801–34809.
43. D'Orso,I. and Frasch,A.C. (2002) TcUBP-1, an mRNA destabilizing factor from trypanosomes, homodimerizes and interacts with novel AU-rich element- and Poly(A)-binding proteins forming a ribonucleoprotein complex. *J. Biol. Chem.*, **277**, 50520–50528.
44. Hartmann,C., Benz,C., Brems,S., Ellis,L., Luu,V.D., Stewart,M., D'Orso,I., Busold,C., Fellenberg,K. *et al.* (2007) The small trypanosome RNA-binding proteins TbUBP1 and TbUBP2 influence expression of F-box protein mRNAs in bloodstream trypanosomes. *Eukaryot. Cell*, **6**(11), 1964–1978.
45. Derbise,A., Lesic,B., Dacheux,D., Ghigo,J.M. and Carniel,E. (2003) A rapid and simple method for inactivating chromosomal genes in Yersinia. *FEMS Immunol. Med. Microbiol.*, **38**, 113–116.
46. Sereno,D. and Lemesre,J.L. (1997) Axenically cultured amastigote forms as an in vitro model for investigation of antileishmanial agents. *Antimicrob. Agents Chemother.*, **41**, 972–976.
47. Papadopoulou,B., Roy,G. and Ouellette,M. (1992) A novel antifolate resistance gene on the amplified H circle of Leishmania. *Embo J.*, **11**, 3601–3608.
48. Salles,F.J., Richards,W.G. and Strickland,S. (1999) Assaying the polyadenylation state of mRNAs. *Methods*, **17**, 38–45.
49. Rochette,A., McNicoll,F., Girard,J., Breton,M., Leblanc,E., Bergeron,M.G. and Papadopoulou,B. (2005) Characterization and developmental gene regulation of a large gene family encoding amastin surface proteins in Leishmania spp. *Mol. Biochem. Parasitol.*, **140**, 205–220.
50. Rafati,S., Hassani,N., Taslimi,Y., Movassagh,H., Rochette,A. and Papadopoulou,B. (2006) Amastin peptide-binding antibodies as biomarkers of active human visceral leishmaniasis. *Clin. Vaccine Immunol.*, **13**, 1104–1110.
51. Wu,Y., El Fakhry,Y., Sereno,D., Tamar,S. and Papadopoulou,B. (2000) A new developmentally regulated gene family in Leishmania amastigotes encoding a homolog of amastin surface proteins. *Mol. Biochem. Parasitol.*, **110**, 345–357.
52. Kundig,C., Haimeur,A., Legare,D., Papadopoulou,B. and Ouellette,M. (1999) Increased transport of pteridines compensates for mutations in the high affinity folate transporter and contributes to methotrexate resistance in the protozoan parasite Leishmania tarentolae. *Embo J.*, **18**, 2342–2351.
53. Bonisch,C., Temme,C., Moritz,B. and Wahle,E. (2007) Degradation of hsp70 and other mRNAs in Drosophila via the 5′ 3′ pathway and its regulation by heat shock. *J. Biol. Chem.*, **282**, 21818–21828.
54. Meijer,H.A., Bushell,M., Hill,K., Gant,T.W., Willis,A.E., Jones,P. and de Moor,C.H. (2007) A novel method for poly(A) fractionation reveals a large population of mRNAs with a short poly(A) tail in mammalian cells. *Nucleic Acids Res.*, **35**, e132.
55. Kushner,S.R. (2002) mRNA decay in Escherichia coli comes of age. *J. Bacteriol.*, **184**, 4658–4665; discussion 4657.
56. LaCava,J., Houseley,J., Saveanu,C., Petfalski,E., Thompson,E., Jacquier,A. and Tollervey,D. (2005) RNA degradation by the exosome is promoted by a nuclear polyadenylation complex. *Cell*, **121**, 713–724.
57. Wyers,F., Rougemaille,M., Badis,G., Rousselle,J.C., Dufour,M.E., Boulay,J., Regnault,B., Devaux,F., Namane,A. *et al.* (2005) Cryptic pol II transcripts are degraded by a nuclear quality control pathway involving a new poly(A) polymerase. *Cell*, **121**, 725–737.
58. West,S., Gromak,N., Norbury,C.J. and Proudfoot,N.J. (2006) Adenylation and exosome-mediated degradation of cotranscriptionally cleaved pre-messenger RNA in human cells. *Mol. Cell*, **21**, 437–443.
59. Hagan,K.W., Ruiz-Echevarria,M.J., Quan,Y. and Peltz,S.W. (1995) Characterization of cis-acting sequences and decay intermediates involved in nonsense-mediated mRNA turnover. *Mol. Cell. Biol.*, **15**, 809–823.
60. Muhlrad,D. and Parker,R. (1994) Premature translational termination triggers mRNA decapping. *Nature*, **370**, 578–581.
61. Liu,H. and Kiledjian,M. (2007) An erythroid-enriched endoribonuclease (ErEN) involved in alpha-globin mRNA turnover. *Protein Pept. Lett.*, **14**, 131–136.